International Journal of Biological Macromolecules 267 (2024) 131564

Contents lists available at ScienceDirect

International Journal of Biological Macromolecules

journal homepage: www.elsevier.com/locate/ijbiomac

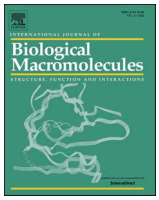

# Ovalbumin interaction with polystyrene and polyethylene terephthalate microplastics alters its structural properties

Nikola Gligorijevic [a,b], Tamara Lujic [a], Tamara Mutic [a], Tamara Vasovic [a], Maria Krishna de Guzman [c,d], Jelena Acimovic [a], Dragana Stanic-Vucinic [a], Tanja Cirkovic Velickovic [a,e,*]

[a] Center of Excellence for Molecular Food Sciences, Department of Biochemistry, University of Belgrade – Faculty of Chemistry, Belgrade, Serbia
[b] Department of Chemistry, University of Belgrade – Institute of Chemistry, Technology and Metallurgy, National Institute of Republic of Serbia, Belgrade, Serbia
[c] Ghent University Global Campus, Yeonsu-gu, Incheon, South Korea
[d] Faculty of Bioscience Engineering, Ghent University, Ghent, Belgium
[e] Serbian Academy of Sciences and Arts, Belgrade, Serbia

ARTICLE INFO

*Keywords:*
Ovalbumin
Microplastics
Polystyrene
Polyethylene terephthalate
Interactions

ABSTRACT

Contaminating microplastics can interact with food proteins in the food matrix and during digestion. This study investigated adsorption of chicken egg protein ovalbumin to polystyrene (PS, 110 and 260 μm) and polyethylene terephthalate (PET, 140 μm) MPs in acidic and neutral conditions and alterations in ovalbumin structure. Ovalbumin adsorption affinity depended on MPs size (smaller > larger), type (PS > PET) and pH (pH 3 > pH 7). In bulk solution, MPs does not change ovalbumin secondary structure significantly, but induces loosening (at pH 3) and tightening (at pH 7) of tertiary structure. Formed soft corona exclusively consists of full length non-native ovalbumin, while in hard corona also shorter ovalbumin fragments were found. At pH 7 soft corona ovalbumin has rearranged but still preserved level of ordered secondary structure, resulting in preserved thermostability and proteolytic stability, but decreased ability to form fibrils upon heating. Secondary structure changes in soft corona resemble changes in native ovalbumin induced by heat treatment (80 °C). Ovalbumin is abundantly present in corona around microplastics also in the presence of other egg white proteins. These results imply that microplastics contaminating food may bind and change structure and functional properties of the main egg white protein.

## 1. Introduction

Ovalbumin (OVA) is one of the major egg proteins, representing 54 % of all egg white proteins [1]. Ovalbumin belongs to the serpin family although it lacks any protease inhibitory activity [2]. It is the only egg white protein with free thiol groups located inside the protein core. Upon denaturation of ovalbumin at 80 °C, free thiol groups become exposed and react with each other, which is the critical step in the formation of egg-white gels [3]. OVA exposed to standard denaturing conditions self-assembles into amyloid nanosheets that elicit immune responses of Th2 type [4]. OVA is also one of the major food allergens. Its allergenicity originates from high structural stability and proteolysis resistance in the gastrointestinal tract [5]. Heat treatment of OVA reduces its allergenic potential and makes it more digestible [6,7]. Heat treatment, however, leads to the loss of food nutritional values, so alternative methods for food processing gain more attention [8]. Techno-functional properties of OVA and egg white, like foaming or making protein networks are essential in the food industry. These properties depend on the OVA structure and its processing [9]. Ovalbumin owns remarkable functional properties, which, together with its great nutritional value, accessibility, abundance, biocompatibility and biodegradability, have made ovalbumin a potent candidate for a wide range of food and pharmaceutical applications, such as for engineering polymeric carriers that can be loaded with bioactive drugs and provide site specific delivery by releasing the cargo at specific sites [10]. However, all ovalbumin functional properties strongly depend on its structure.

Microplastic particles (MPs) represent major pollutants today,

* Corresponding author at: Center of Excellence for Molecular Food Sciences, Department of Biochemistry, University of Belgrade, Faculty of Chemistry, Studentski trg 12-16, Belgrade, Serbia.
*E-mail address:* tcirkov@chem.bg.ac.rs (T. Cirkovic Velickovic).

https://doi.org/10.1016/j.ijbiomac.2024.131564
Received 29 December 2023; Received in revised form 9 April 2024; Accepted 10 April 2024
Available online 16 April 2024

affecting both the water and land environment. These particles are formed as a consequence of chemical, biological and mechanical degradation of plastic waste, but the main source of MPs contaminating food seems to be food packaging [11–13]. MPs is also found in eggs with a quantity of about 11.67 particles per egg. Most of the found MPs had spherical shapes and were of size range from 50 to 100 μm. In addition, the abundance of MPs was larger in egg yolks compared to egg whites [14]. On the other hand, a study using commercial $^{14}C$ labeled polystyrene microplastic that was fed to the chickens, resulted in this microplastic being distributed mainly in feces and lower quantities being found in eggs and blood [15].

Even though MPs are highly distributed in nature, the exact risks they have on living organisms and the molecular mechanisms of their potential harmful effects are still not fully known [16]. We need to better understand interactions of food proteins with the novel food contaminant and impact on protein structure and functional properties.

Biomolecules, including proteins, are able to form biofilms on the surface of MPs. This process usually involves several steps, including the initial binding of biomolecules and the formation of the initial protein corona. Molecules with higher affinity bind more strongly and form a hard corona. Onto hard corona, soft corona may form as the last step [17]. The coating of MPs with biomolecules significantly impacts biological effects of MPs [18,19]. There has been a lot of research in the field of protein-nanoparticles interactions, upon which recent studies having the process of adsorption and corona formation of proteins onto MPs (as well as smaller plastic particles, nanoplastics) can build upon [11,20,21]. Challenges faced in these studies are related to the heterogeneity of the MPs, particularly found in the environment, from the aspect of size, shape, chemistry, additives present, as well as propensity to get chemically modified during the aging process in the environment [22,23].

Only several studies characterized the direct binding of proteins to MPs, and mostly from the aspects of human health risks. Human serum albumin (HSA) was found to interact with polyvinyl chloride (PVC) MPs of around 5 μm in size. These interactions lead to a decrease in the α-helical content of HSA [20]. SDS-PAGE analysis of protein corona formed onto the surface of MPs isolated from circulation showed that this corona is mainly formed from HSA, globulins and fibrinogen, which may influence thrombus formation [24]. Recent study showed that pepsin interacts with polystyrene microplastics and this interaction leads to structural altercations of pepsin, inhibition of pepsin activity and impairment of digestion of milk proteins in simulated gastric conditions [25]. It was demonstrated that simulated digestive fluids do not decompose MPs (polyethylene (PE), polypropylene (PP), PVC, polyethylene terephthalate (PET) and polystyrene) neither modify their shapes and sizes, but protein coronae formed on the surface of these particles, may affect their properties [26]. In vitro small intestinal epithelium model showed that PE MPs increased fat digestion, with corona being dominantly composed of triacylglycerols and enzyme triacylglycerol lipase. Observed findings proposed digestion of triacylglycerol by lipase on the surface of lipid-coated MNPs as a potential mechanism [27].

Given the frequent occurrence of MPs in food and beverages, ingestion as a major exposure route of humans to MPs, and a limited knowledge on interactions and impact of MPs on structure and functional properties of specific food proteins, we addressed this question in this study by investigating adsorption of egg white protein ovalbumin on two types of MPs (PS and PET) of different sizes at different pH (pH 3 and pH 7).

However, literature data on MPs-induced structural changes of food proteins upon their adsorption on MPs surface, and particularly at different pH, are still scarce. Therefore, the objective of this study was to investigate the interactions of ovalbumin with PS and PET MPs and the effects of these interactions on ovalbumin structural properties. MPs used were made by milling and sieving that have irregular shapes and wider size ranges, which much better corresponds to what can be found in nature [12]. The influence of tested MPs on OVA structure, its corona formation on MPs surface and the effect of thermal treatment on MPs-exposed OVA structure, stability and fibril formation were investigated. Binding of OVA to the MPs was also investigated in the presence of other egg white proteins by monitoring corona formation.

## 2. Materials and methods

All reagents were purchased from Sigma and were of analytical grade. Microplastics were prepared by the Center of Polymer and Material Technologies of the Department of Materials, Textiles and Chemical Engineering, Ghent University, by a controlled-milling process using polystyrene (Styrolution PS 124N) and polyethylene terephthalate (Lighter™ C93 PET) and a variable speed rotor mill (Pulverisette 14, Fritsch, Germany) with two different sieve ring sizes of 120 μm and 500 μm. Two PS fractions (designated "large" and "small") and one PET fraction (designated "small") were collected and used in experiments. Before use, microplastics were kept at 4 °C as a dry powder. Microplastics were characterized by Raman spectrometry for their identity (**Section S1, Fig. S1**) and microFTIR for their shapes and sizes (**Section S1, Figs. S2 and S3, Table S1**). Raman spectroscopy confirmed MPs identities (**Fig. S1**). The shapes of MPs are mostly spheres and spheroids with some fragments, while there were no fibers (**Fig. S2**). The length of large PS MPs was in the range 95–870 μm (average 260 μm, median 197), for small PS in the range 43–178 μm (average 112, median 120 μm), and for small PET in the range 44–321 μm (average 143, median 125) (**Fig. S3 and Table S1**).

Ovalbumin was isolated and purified according to a previously published method, with minor modifications [28] and its purity was confirmed by reducing SDS-PAGE electrophoresis (**Section S2, Fig. S4**).

### 2.1. Binding analysis of ovalbumin to microplastics

Unless otherwise stated, all incubations were performed at room temperature with reaction volumes of 1 mL. Two buffers were used, 20 mM phosphate buffer pH 7 and 20 mM glycine buffer pH 3.

Previous to performing the binding experiment for affinity calculation, equilibration time points for ovalbumin binding to tested microplastics under both pH conditions were determined (**Section S3, Fig. S5**). This was done by incubating 2 mg/mL of ovalbumin to 20 mg of each microplastic type. Reaction mixtures were constantly mixed on a rotator at room temperature. Microplastic particles were separated from the supernatant by centrifugation at 13000 rpm (MiniSpin centrifuge, Eppendorf, Hamburg, Germany) and further filtration using 0.22 μm filters (PVDF protein low-binding, Durapore, Merck). Absorbances of supernatants at 280 nm were measured at the beginning of the experiment and after 1, 2, 4 and 19 h of reaction. The theoretical extinction coefficient for ovalbumin, $\varepsilon_{1\%} = 7.16$, was used to calculate its concentration [29].

For affinity constant calculation, five different concentrations of ovalbumin were incubated to a fixed mass of microplastic (20 mg). Concentrations used were 0.25, 0.35, 0.5, 1 and 2 mg/mL. Reactions were constantly mixed on a rotator at room temperature. When equilibration time was reached, 4 h for all tested conditions and microplastic, reaction mixtures were centrifuged, filtrated and absorbance at 280 nm was measured as previously explained. Obtained data were fitted using Langmuir, Freundlich, Redlich–Peterson (RP) and Guggenheim–Anderson–de Boer (GAB) adsorption models. Fitting and binding parameters were obtained using Origin software by non-linear regression analysis.

For Langmuir adsorption isotherm, the following equation was used:

$$Qe = \frac{Qm \times KL \times Ce}{1 + KL \times Ce} \quad (1)$$

Where Qe (mg/g) is the mass of adsorbed protein per gram of micro-

plastic at equilibrium, Ce (mg/L) is the concentration of unbound protein in solution at the equilibration point, $Q_L$ (mg/g) is the maximum amount of adsorbed ovalbumin per mass unit of MPs and $K_L$ (mL/mg) is Langmuir constant.

From the Langmuir model, the separation factor or equilibrium parameter ($R_L$) is calculated using the following equation:

$$RL = \frac{1}{1 + KL \text{ x } C0}, \quad (2)$$

where $K_L$ is the Langmuir constant and $C_0$ is the highest initial concentration of ovalbumin used.

For Freundlich adsorption isotherm, the following equation was used:

$$Qe = K_F \times Ce^N, \quad (3)$$

where N is dimensionless reaction order and represents the measure of heterogeneity and $K_F$ ((mg/g)*(mL/mg)$^{1/n}$) is the Freundlich constant.

For RP adsorption isotherm, the following equation was used:

$$Qe = \frac{KR \text{ x } Ce}{1 + \alpha Ce\beta}, \quad (4)$$

where $K_R$ (mL/mg) is Redlich−Peterson constant, α is a constant in mL/mg and β is an exponent that usually ranges from 0 to 1. If it is close to 1, the model approaches the Langmuir isotherm and if it is close to 0, it approaches the Freundlich model.

For GAB adsorption isotherm, the following equation was used:

$$Qe = \frac{QG \text{ x } Khard\ G \text{ x } Ce}{(1 - Ksoft\ G \text{ x } Ce)(1 + Khard\ G - Ksoft\ G \text{ x } Ce)}, \quad (5)$$

where $Q_G$ (mg/g) is the surface concentration of strongly adsorbed protein, $K_{hard\ G}$ (mL/mg) is the adsorption constant for the hard corona and $K_{soft\ G}$ is the adsorption constant for the soft corona.

### 2.2. Circular dichroism (CD) spectrometry analysis of ovalbumin in the presence of microplastics

The influence of microplastic on the structure of ovalbumin was tested by CD spectrometry. For this purpose, 1.3 mg/mL of ovalbumin was incubated in the presence of 20 mg/mL of all three types of microplastic on both pH 3 and pH 7, at room temperature, under constant mixing on rotator. Immediately after mixing the two components, microplastic was removed from the mixture, as explained in Section 2.1 and CD spectra of ovalbumin in the supernatant were recorded. This was the 0 h time point. The same procedure was done after 1, 2 and 4 h of incubation, as well, for observation of structural changes of ovalbumin during the time interval it needs to reach binding equilibrium. As a control, spectra of ovalbumin without microplastic were recorded in the same time intervals. The secondary structure of ovalbumin was monitored by recording far-UV CD spectra in the wavelength region from 190 to 260 nm, while the tertiary structure was monitored by recording near-UV CD spectra in the wavelength region from 260 to 320 nm. Signals originating from corresponding buffers were subtracted from obtained spectra of ovalbumin. Spectra were normalized by presenting results as molar ellipticity. Obtained far-UV CD spectra were further analyzed by the CDpro software package, using the CONTIN algorithm, to calculate secondary structure motifs. SP29 database was used for the analysis.

### 2.3. Analysis of soft and hard corona formation by isolated ovalbumin on the surface of MPs

Soft and hard ovalbumin corona on MPs were isolated from separated MPs samples, previously incubated for 4 h and used for CD spectrometry analysis, using the procedure of Magri et al. [30]. Pelleted microplastics, from which supernatants were removed, were washed three times with distilled water (200 μL each time) to remove soft corona from the microplastic. Each time, pellets were vortexed for 30 s, incubated for 5 min in water, pelleted and supernatants were removed and kept for analysis. After three cycles of water washing, Laemmli buffer was added to microplastic pellets to obtain OVA from the hard corona. These mixtures were incubated for 10 min at 95 °C, with constant shaking. All of the samples were analyzed by reducing SDS-PAGE using 12 % gel. The gels were stained with Coomassie Brilliant Blue (CBB) and scanned using Typhoon™ FLA 7000 biomolecular Imager (Cytiva, USA). Protein bands were analyzed by densitometry using ImageQuant software and subject to MS analysis as described in detail in section S4 in Supplementary material.

### 2.4. Analysis of soft and hard corona formation by egg white protein extract on the surface of MPs

Egg white extract was prepared according to published procedure [28]. One egg white was mechanically separated from egg yolk. To 35 mL of egg white 105 mL of 100 mM NaCl was added and the extract was homogenized for 1 h while gently mixing on a magnetic stirrer. The pH of the homogenate was adjusted to 6 and stirred for another 30 min. Ovomucin was left to precipitate at 4 °C overnight. The next day the precipitated ovomucin was separated by centrifugation at 5000 ×*g* for 20 min at 4 °C. Concentration of protein in the extract was determined with a BCA assay (Pierce, Thermo Fisher Scientific, USA) to be 28.5 mg/mL.

The concentration of the egg white extract was adjusted to 1.3 mg/mL, as with previous experiments, using a 20 mM phosphate pH 7 or 20 mM glycine pH 3 buffer. To 20 mg of MPs 1 mL of diluted extract was added. MPs were incubated with the extract for 4 h at room temperature with constant rotation. Soft and hard coronas were obtained as previously described in Section 2.3. All samples were analyzed by reducing SDS-PAGE using 12 % gel (Hoefer Scientific Instruments, USA). For the controls 10 μL was placed in wells, and for the samples 30 μL. The gels were stained with Coomassie Brilliant Blue (CBB) and scanned using Typhoon™ FLA 7000 biomolecular Imager (Cytiva, USA). Protein bands were analyzed by densitometry using ImageQuant software.

### 2.5. Influence of thermal treatment on the structure of bulk and ovalbumin from soft corona obtained from small PET and small PS, at pH 7

For the next three experiments, the samples of bulk and soft corona ovalbumin were prepared as described in Section 2.3 and further treated as described in the following sections.

#### 2.5.1. Structural analysis by CD spectrometry

Far-UV CD spectra of all ovalbumin samples, 200 μL, in final concentrations of 0.1 mg/mL were recorded using the cuvette with optical path length of 1 mm at 25 °C. Spectra were recorded as described in Section 2.2 using the same equipment. After recording of CD spectra, samples were incubated for 10 min at 80 °C with shaking at 350 rpm using thermo shaker TS-100 (BioSan, Latvia). After thermal treatment, samples were cooled to 25 °C and far-UV CD spectra were recorded again. Signals originating from corresponding buffers were subtracted from obtained spectra of ovalbumin. Spectra were normalized by presenting results as molar ellipticity. Obtained far-UV CD spectra were further analyzed by the CDpro software package, using the CONTIN algorithm, to calculate secondary structure motifs. SP29 database was used for the analysis.

#### 2.5.2. Thioflavin T (ThT) assay

Fluorescence emission of ThT alone and in the presence of OVA samples was measured by excitation of ThT at 435 nm and recording emission at 485 nm. ThT was added at final concentration of 20 μM to prepared OVA samples (0.05 mg/mL, final concentration). Fluorescence

signals were first recorded unheated at room temperature using a FluoroMax-4 spectrofluorimeter (Horiba Scientific, Japan) with excitation and emission slits set at 5 nm. Samples were then treated thermally in the same way as in Section 2.5.1, cooled to 25 °C following the addition of ThT and recording of its emission again. Obtained spectra were corrected by subtracting emission spectra from appropriate controls without ThT.

#### 2.5.3. Determination of temperature stability

Thermal stability, indicated by melting temperature (Tm), was determined by spectrofluorimetry using FluoroMax®-4 spectrofluorimeter (Horiba Scientific, Japan), with Peltier element. The thermal stability of ovalbumin samples were recorded in the temperature range from 25 to 89 °C. Temperature increment was 2 °C/min and equilibration time was set to be 1 min. Ovalbumin samples, with a final concentration of 400 nM, were excited at 280 nm and emission spectra were recorded in the range from 300 to 400 nm. Melting curves were plotted as a reduction of emission maxima at 338 nm with temperature. Data were fitted into sigmoidal curves with inflection points representing Tm.

#### 2.5.4. Digestion analysis

Digestion procedure is explained in Supplementary material, Section S5.

### 2.6. Statistical analysis

The data are presented as the mean ± S.D. Unless otherwise stated, all experiments were conducted two times. Data were analyzed using one-way ANOVA with Tukey's multiple comparison test at a significance level of 0.05.

## 3. Results

### 3.1. Binding analysis of ovalbumin to microplastic particles

The equilibration time point, at which processes of adsorption and desorption of molecules on the adsorbent are at equilibrium, is the time point used for calculating affinity constants. Regarding ovalbumin and three tested microplastics, small PET, small PS and large PS, the equilibration time was determined to be 4 h, **Fig. S5**. This equilibration time was the same at both pH 3 and pH 7.

Adsorption equilibrium data, which express the relationship between the mass of OVA adsorbed per unit weight of MPs at equilibrium (Qe) and OVA equilibrium concentration in solution (Ce), were obtained. Experimental adsorption isotherms were analyzed by Langmuir, Freundlich, RP, as well as GAB isotherms, by non-linear regression analysis.

**Fig. S6.** shows the fit of the isotherm models to the experimental data for the adsorption of OVA onto MPs. Obtained isotherms are characterized by a large increase in the amount adsorbed at low concentrations, followed by a lower increase and finally by a plateau at high concentrations. It could be observed that in the case of OVA adsorption at small MPs (**Fig. S6. A, B, C and D**) Qe increase with Ce increase is more pronounced than with large MPs (**Fig. S6. E and F**). Saturation is reached at lower OVA concentration, presumably because of the higher available surface per mass unit. In contrast to PS MPs isotherms (**Fig. S6. C, D, E and F**), both PET MPs isotherms tend to demonstrate biphasic curves (**Fig. S6. A and B, third point**). At pH 7 the best fitting was obtained for RP isotherm, and at pH 3 GAB and RP isotherms, while Freundlich was less favorable.

Langmuir, Freundlich, RP and GAB isotherms constants for the adsorption of OVA onto MPs are shown in Table 1. Nonlinear regression analysis was used as, in comparison to linear regression analysis, this method does not transform data sets and thus no distortions are created in the original error distribution. The best correlation coefficients were obtained for PR isotherms, while the lowest correlation was obtained for Freundlich isotherms.

$K_L$ (Langmuir constant), $K_R$ (Redlich−Peterson constant) and $K_{hard\ G}$ (adsorption constant for the hard corona) are measures of OVA affinity toward MPs. According to Langmuir constant ($K_L$), In general, OVA has higher affinity for PS MPs than for PET MPs, affinity is higher at pH 3 for all MPs, and at pH 7 OVA affinity is higher for MPs with smaller surface per mass (large PS). Similarly, based on RP constant, OVA affinity is higher at pH 3, and at pH 7 affinity is higher for MPs with smaller surface per mass. However, higher affinity was obtained for PS than for PET only at pH 3, and the difference between pH 3 and pH 7 is more drastic (for small PS even two orders of magnitude higher). It should be mentioned that although the size of small PS is slightly lower than size of small PET, thus having a slightly higher surface, the difference in their affinity is dominantly due to difference in type of plastic and only partly due to difference in surface. In contrast to Langmuir isotherm, RP isotherm gives a pronounced difference between the affinity of small PS and large PS at pH 3, where small PS has a higher affinity for an order of magnitude. Although it was not possible to reliably get parameters for GAB isotherms at pH 7, at pH 3 a similar trend was obtained as for Langmuir and RP isotherms. Moreover, $K_{hard\ G}$ values are similar to $K_L$ values at pH 3. Similarly to RP isotherms, from GAB isotherm difference between affinity of small PS and large PS at pH 3 is observable, where PS MPs

**Table 1**
Langmuir, Freundlich, Redlich−Peterson and Guggenheim−Anderson−de Boer (GAB) isotherms constants for the adsorption of OVA onto MPs obtained by nonlinear regression analysis. n/a – it was not possible to reliably get parameters for GAB isotherms at pH 7. $K_L$ - Langmuir constant, $Q_L$ - maximum amount of adsorbed protein, $R_L$ - Langmuir equilibrium parameter, $K_F$ - Freundlich constant (adsorption capacity), n - characterizes the heterogeneity of the system, KR - Redlich−Peterson constant, α and β – constant and exponent in Redlich−Peterson equation, $Q_G$ - surface concentration of strongly adsorbed protein, $K_{hard}$ G -adsorption constant for the hard corona, $K_{soft}$ G -adsorption constant for the soft corona, $R^2$ - coefficient of determination for corresponding isotherm curves.

| Isotherm model | Parameters of isotherms | Small PET pH 7 | Small PET pH 3 | Small PS pH 7 | Small PS pH 3 | Large PS pH 7 | Large PS pH 3 |
|---|---|---|---|---|---|---|---|
| Langmuir | $K_L$ (mL/mg) | 1.2 | 6 | 1.4 | 10 | 4 | 10 |
| | $Q_L$ (mg/g) | 8.34 | 9.26 | 11.11 | 26.75 | 3.81 | 4.36 |
| | $R_L$ | 0.294 | 0.077 | 0.263 | 0.048 | 0.111 | 0.048 |
| | $R^2$ | 0.83 | 0.93 | 0.97 | 0.975 | 0.86 | 0.99 |
| Freundlich | $K_F$ ((mg/g)*(mL/mg)$^{1/n}$) | 4.26 | 7.59 | 5.98 | 23.73 | 2.86 | 3.88 |
| | n | 1.988 | 4.608 | 1.972 | 4.098 | 3.745 | 7.936 |
| | $R^2$ | 0.78 | 0.88 | 0.9 | 0.96 | 0.66 | 0.87 |
| Redlich − Peterson | $K_R$ (mL/mg) | 8.55 | 62.0 | 6.22 | 425 | 8.85 | 42.5 |
| | α (mL/mg) | 0.00155 | 8.7 | 1.25E-06 | 35 | 0.0569 | 8.7 |
| | β | 1.856 | 0.965 | 2.724 | 0.89 | 1.486 | 1.014 |
| | $R^2$ | 0.995 | 0.896 | 0.807 | 0.992 | 0.972 | 0.983 |
| Guggenheim–Anderson–de Boer | $Q_G$ (mg/g) | n/a | 9.179 | n/a | 23.2 | n/a | 4.399 |
| | $K_{hard\ G}$ (mL/mg) | n/a | 6.000 | n/a | 13.913 | n/a | 10.268 |
| | $K_{soft\ G}$ (mL/mg) | n/a | −0.004 | n/a | 0.086 | n/a | −0.004 |
| | $R^2$ | n/a | 0.893 | n/a | 0.989 | n/a | 0.981 |

with higher surface per mass have higher affinity.

Reliable $K_{soft\ G}$ was obtained only for small PS at pH 3, most likely due to the highest affinity. $K_{hard\ G}$ value for small PS at pH 3 is for about two orders of magnitude higher than $K_{soft\ G}$. Studies using GAB isotherm for protein binding to silica nanoparticles observed difference between $K_{hard\ G}$ and $K_{soft\ G}$ for several orders of magnitude [31,32]. Such low $K_{soft\ G}$ implies that OVA molecules in soft corona easily desorb to bulk solution. Ratio of $K_{hard\ G}$ / $K_{soft\ G}$, presenting a measure of adsorption from soft corona to hard corona, is very high (about 160), implying very low desorption of OVA molecules from hard corona to soft corona due to strong OVA binding in hard corona.

$Q_L$ (maximum amount of adsorbed protein), $K_F$ (Freundlich constant, adsorption capacity) and $Q_G$ (surface concentration of strongly adsorbed protein) are measures of adsorption capacity of MPs for OVA. Based on $Q_L$ it can be observed that adsorption capacity is higher for MPs with higher surface per mass (small PS and small PET), adsorption capacity is higher for PS than for PET, adsorption capacity is higher at pH 3 than at pH 7 and adsorption capacity is the highest for small PS at pH 3. As mentioned above, the adsorption capacity of small PS than small PET is mainly due to difference in MPs type and less due to slightly higher surface area of small PS. Similar trend is observable according to Freundlich constant, except that differences at pH 3 and pH 7 are more drastic (for about order of magnitude) and at pH 7 adsorption capacity is higher for MPs with smaller surface per mass (large PS). It should be mentioned that each $K_F$ is lower than the corresponding value of $Q_L$ as $K_F$ is not a measure of the total adsorption capacity, but should be considered as a comparative measure of the adsorption under specified conditions [33]. At pH 3 $Q_G$ values from GAB isotherm are very similar to $Q_L$ values from Langmuir isotherm (9.179 vs 9.26, 23.2 vs 26.75 and 4.399 vs 4.36).

Freundlich isotherm implies that tested OVA-MPs are heterogeneous systems, as for all MPs n values are higher than 1. Heterogeneity is higher for MPs with lower surface per mass (large PS) and it is higher at pH 3 than pH 7, but heterogeneity does not depend on MPs type. Adsorption heterogeneity is most likely due to multilayer adsorptions. Values $1 < n < 10$ indicate that OVA is favorably adsorbed by all MPs, but adsorption is not linear, e.g. there is decrease in the interaction between the MPs and OVA with the increase in OVA density on MPs surface. In RP isotherm β values at pH 3 are near 1, suggesting that at pH 3 experimental isotherms are approaching more Langmuir than Freundlich isotherm. Calculated $R_L$ values, Langmuir equilibrium parameter, is $0 < R_L < 1$ for all tested MPs, implying that adsorption is favorable. However, it could be observed that at pH 3 interactions are much stronger than at pH 7, going toward 0, e.g. toward irreversible adsorption.

### 3.2. Influence of microplastic on the structure of bulk ovalbumin after its incubation with MPs

Far UV, Fig. 1, and near UV, Fig. 2, CD spectra were recorded in OVA samples after its incubation for 1 h, 2 h, 3 h and 4 h without and with MPs at pH 3 and pH 7. Far UV CD spectra were further analyzed using the CDpro software package (Table 2).

From far UV CD spectra of OVA at pH 7, a minimum could be observed at around 222 nm and a shoulder at 208 nm, consistent with the typical OVA native secondary structure containing a mixture of α-helix and β-sheet structures [34]. Depending on pH, presence or absence of MPs, type and size of MPs, as well as the time of incubation, there are slight changes in OVA secondary structure. These changes are more observable in far UV CD spectra (inserts in Fig. 1) and calculated secondary structure content presented in Table 2. Although there are slight secondary structure changes even in OVA alone when incubated at pH 7, these changes are more pronounced in the presence of MPs. In the presence of all MPs, at both pH, the first change of secondary structure occurs as a β to α transition. Depending on MPs and pH, it happens at different incubation time, lasts for a shorter or longer time and transitions to different extent. This transition starts at 1 h, except for small PS at pH 3, where the β to α transition happens already at 0 h. β to α transition is followed by α to β transition in all samples except large PS at pH 7. These results suggest that the presence of MPs potentiates OVA secondary structure changes, particularly small PS.

In contrast to secondary structure, OVA tertiary structure changes are more dramatic, again depending on pH, presence or absence of MPs, type and size of MPs, as well as time of incubation. Conformational changes of OVA alone during incubation up to 4 h could be observed at both pH. However, in the presence of MPs conformational changes are much more pronounced. In comparison to OVA alone at pH 3, in the presence of all MPs at pH 3 there is decreased near UV CD signal, suggesting that aromatic amino acid residues loose fixed asymmetric environment, particularly Tyr and Trp residues. This implies loosening of tertiary structure, e.g. destabilization of OVA conformation. This destabilization was most pronounced in the presence of small PET after 2 h and 4 h, as well as in the presence of large PS after 4 h. In contrast, at pH 7 in the presence of MPs there is an increase of near UV CD signal, in comparison to OVA alone at pH 7, demonstrating that Phe, Tyr and Trp residues are in a more fixed asymmetric environment. This implies that the presence of MPs induces a more ordered tertiary structure. This stabilization of tertiary structure was most pronounced in the presence of large PS after 2 h and 4 h, and particularly in the presence of small PS after 4 h.

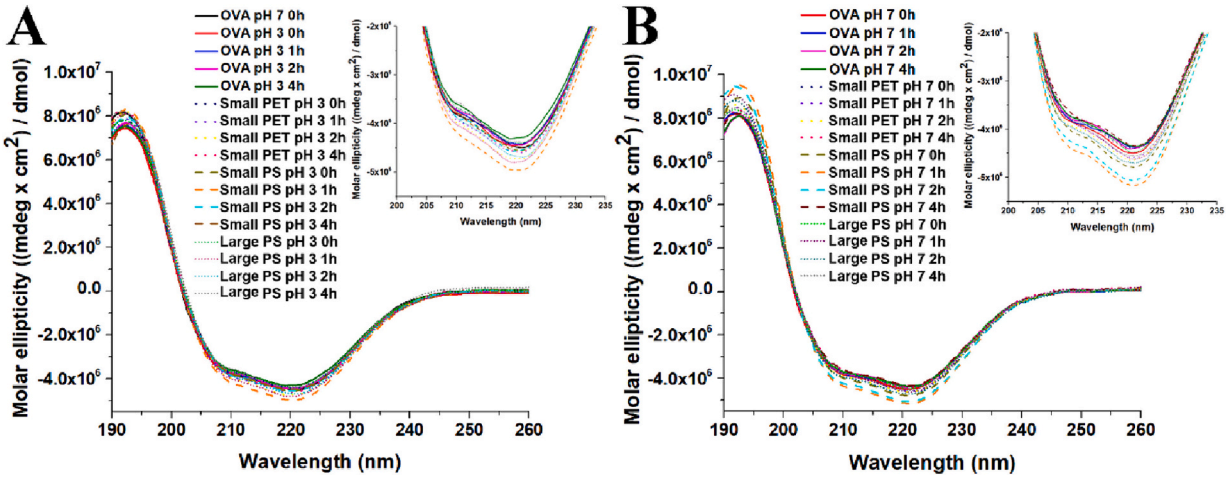


**Fig. 1.** Far UV CD spectra of ovalbumin (OVA) samples after incubation for 1 h, 2 h, 3 h and 4 h without and with microplastics (MPs) at pH 3 (A) and pH 7 (B). Inserts represent zoom out of region 200–235 nm. OVA pH 7 at 0 h is native OVA.

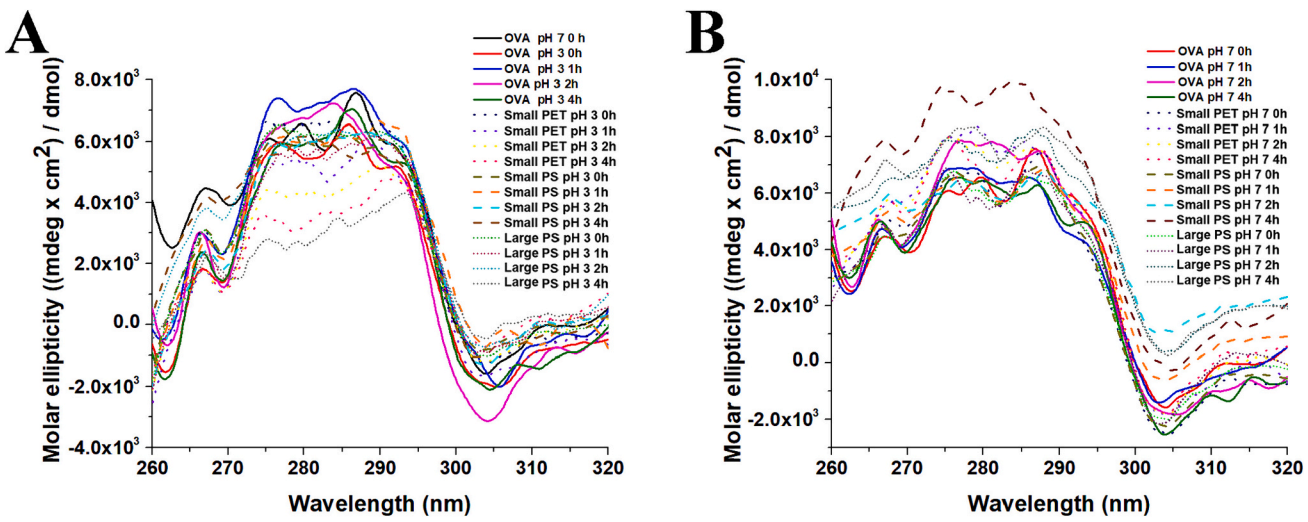


**Fig. 2.** Near UV CD spectra of ovalbumin (OVA) samples after incubation for 1 h, 2 h, 3 h and 4 h without and with MPs at pH 3 (A) and pH 7 (B). OVA pH 7 at 0 h is native OVA.

**Table 2**
Calculated content (%) of secondary structure motifs in OVA samples incubated with or without MPs using the CDpro software package.

| | Time (h) | α-helix | β-sheet | Turn | Random |
|---|---|---|---|---|---|
| pH 3 | | | | | |
| OVA alone | 0 | 31.3 | 17.2 | 22.1 | 29.2 |
| | 1 | 30.6 | 18.1 | 21.6 | 26.7 |
| | 2 | 31.4 | 18.1 | 21.3 | 29.1 |
| | 4 | 29.9 | 19.1 | 21.7 | 29.3 |
| OVA + small PET | 0 | 30.8 | 19 | 21 | 29.2 |
| | 1 | 30.8 | 19 | 21 | 29.2 |
| | 2 | 32.7 | 17.6 | 20.4 | 29.4 |
| | 4 | 31.9 | 18.3 | 20.7 | 29.2 |
| OVA + small PS | 0 | 31.8 | 18.3 | 20.9 | 29.1 |
| | 1 | 34 | 15.9 | 21.2 | 28.9 |
| | 2 | 31.9 | 17.8 | 21.3 | 29 |
| | 4 | 31.7 | 17.2 | 22.2 | 29 |
| OVA + large PS | 0 | 30.8 | 18.7 | 21.1 | 29.4 |
| | 1 | 33.1 | 16.8 | 21.1 | 29 |
| | 2 | 32.1 | 17.4 | 21.3 | 29.2 |
| | 4 | 31 | 19.6 | 20.3 | 29.3 |
| pH 7 | | | | | |
| OVA alone | 0 | 32.3 | 18 | 20.8 | 29 |
| | 1 | 31.8 | 18.9 | 20.5 | 28.9 |
| | 2 | 32.1 | 18 | 21.1 | 28.8 |
| | 4 | 32 | 17.5 | 21.3 | 29.3 |
| OVA + small PET | 0 | 31.4 | 18.9 | 20.3 | 29.4 |
| | 1 | 32.7 | 17.4 | 20.4 | 29.4 |
| | 2 | 33.3 | 17.5 | 20.1 | 29 |
| | 4 | 31.7 | 18.7 | 20.3 | 29.3 |
| OVA + small PS | 0 | 34.3 | 16.9 | 19.9 | 28.8 |
| | 1 | 36.4 | 15.4 | 19.6 | 28.5 |
| | 2 | 35.2 | 16 | 19.5 | 29.2 |
| | 4 | 31.3 | 19 | 20.6 | 29.1 |
| OVA + large PS | 0 | 31.6 | 18.6 | 20.2 | 29.6 |
| | 1 | 33 | 18.3 | 19.2 | 29.4 |
| | 2 | 33.7 | 17.3 | 20.2 | 28.8 |
| | 4 | 34.5 | 18 | 20 | 29.5 |

### 3.3. Soft and hard corona formation of ovalbumin on the surface of MPs

Analysis of protein corona shows that ovalbumin is capable of forming both soft and hard corona onto the surface of all three tested MPs, after 4 h of incubation, Fig. 3. This was also observed at both pH 3 and pH 7. Besides the ovalbumin band, additional protein bands could be observed, especially in hard corona, lanes 4, formed at pH 7 onto the surface of small PET and small PS, where they accounted for about 50 % of the entire protein amount, as determined by densitometry. While these protein bands are almost not observable in control ovalbumin preparation (Lanes marked as Ctrl on Fig. 3), it seems that they were concentrated by MPs, and thus their appearance became stronger. This also indicates that they have higher preferences for the interaction with the tested MPs, compared to OVA. Protein bands other than full length OVA from hard corona of small PS (Fig. 4A, lane 4 at pH 7) were analyzed by mass spectrometry (**Section S4, Fig. S7**). The band, approximately 40 kDa in size, is predominantly composed of ovalbumin (OVA) along with minor quantities of ovomucoid, ovotransferrin, protein TENP, and OVA-related proteins. The other bands are solely composed of OVA, indicating that all bands present in the hard corona are essentially fragments of OVA. As protein fragments are partially or fully unfolded, they have higher levels of exposed hydrophobic patches, resulting in higher affinity for MPs surface in comparison to intact OVA having folded conformation. On the other hand, soft corona is made almost exclusively from intact, full length, protein.

### 3.4. Influence of thermal treatment on the structure of soft corona ovalbumin

Soft corona ovalbumin was isolated from PS and PET MPs and subject to characterization of secondary and tertiary structure changes by CD spectroscopy, at room temperature and after thermal treatment at 80 °C. OVA remaining in solutions after separation of MPs (bulk OVA), as well as OVA not exposed to MPs were analyzed in addition. Far-UV CD spectra of OVA samples before and after thermal treatment are presented in Fig. 4A. At room temperature, the secondary structure of OVA forming the soft corona on both PET and PS MPs is pronouncedly altered compared to control sample and corresponding bulk ovalbumin. This change is reflected in decrease in α-helices and increase in β-sheets and turns, e.g. α to β transition, which was more pronounced in PET soft corona (Table 3). Thermal treatment for 10 min at 80 °C induced structural alterations of OVA in all analyzed samples, with α to β transition (Fig. 4A). However, this α to β transition was dramatic in both PET and PS soft corona, where α-helices were reduced to half and β-sheet increased twice of their content in native OVA, but without changes in random coil. These results suggest that in soft corona at both room temperature and after short heat treatment, the level of ordered secondary structures is completely preserved, but with rearrangement of α-helices and β-sheets, which was more dramatic after heat treatment. It

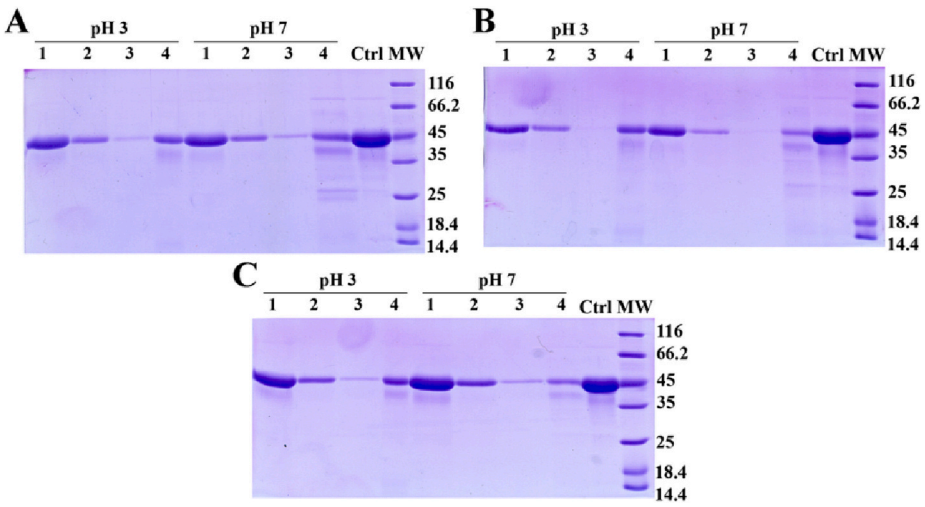


**Fig. 3.** Formation of soft and hard corona by ovalbumin on the surface of small polyethylene terephthalate (PET) (A), small polystyrene (PS) (B) and large polystyrene (PS) (C) at pH 3 and 7. Lanes 1–3: ovalbumin from soft corona, lanes 4: ovalbumin from hard corona, Ctrl: control ovalbumin incubated without microplastics (MPs), MW: molecular weight markers.

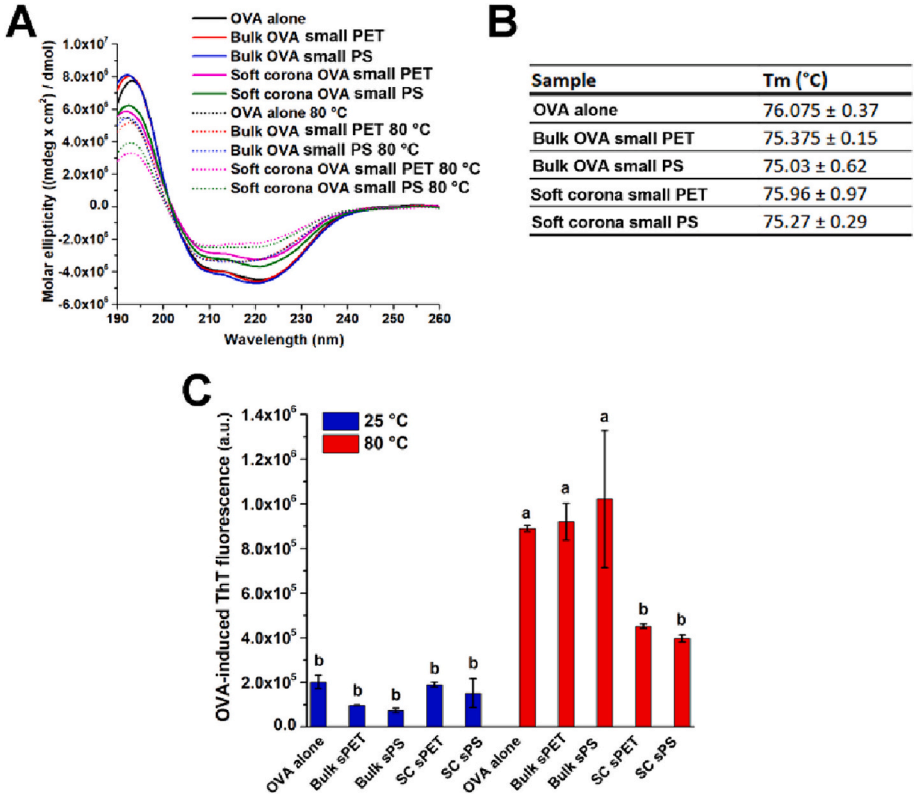


**Fig. 4.** Far CD spectra of control, bulk and soft corona ovalbumin (OVA) samples before and after heating for 10 min at 80 °C. Bulk and soft corona OVA were made by incubation with small polystyrene (sPS) and small polyethylene terephthalate (sPET) (A). Melting point (Tm) values of control, bulk and soft corona OVA samples (B). Intensity of thioflavin T (ThT) emission measured at 485 nm of control, bulk and soft corona OVA samples before and after heating for 10 min at 80 °C (C). Means with different letters (a-b) have significant differences ($p < 0.05$).

could also be observed that the content of secondary structure in soft corona of both MPs at 25 °C is similar to thermally treated OVA and bulk fraction of OVA, implying that conformational changes in soft corona resemble conformational changes induced by heat treatment.

### 3.5. Thermal stability of OVA exposed to MPs

Examination of thermal stability of OVA by spectrofluorimetry demonstrated that its incubation with both types of MPs (PS, PET, small size) has no effect on OVA in both bulk fraction and soft corona (Fig. 4B). Melting point of all samples was about 75 °C. Thus, MPs-induced conformational changes with completely preserved level of ordered secondary structures have as a consequence retained thermal stability of OVA.

**Table 3**
Calculated content (%) of secondary structure motifs in ovalbumin samples at 25 °C and after heating at 80 °C for 10 min using the CDpro software package.

| | α helix | β sheets | turns | random |
|---|---|---|---|---|
| 25 °C | | | | |
| OVA | 33.6 | 14.2 | 22.5 | 29.7 |
| Bulk OVA small PET | 33.5 | 16 | 21.3 | 29.2 |
| Bulk OVA small PS | 33.9 | 16.3 | 20.8 | 29.1 |
| Soft corona OVA small PET | 23.5 | 25.6 | 21.4 | 29.5 |
| Soft corona OVA small PS | 28.5 | 17.5 | 24.2 | 29.9 |
| 80 °C | | | | |
| OVA | 23.9 | 25.7 | 21.3 | 29.2 |
| Bulk OVA small PET | 23.9 | 24.8 | 22.2 | 29.1 |
| Bulk OVA small PS | 24.3 | 24.8 | 21.8 | 29 |
| Soft corona OVA small PET | 16.8 | 31.4 | 22.7 | 29.1 |
| Soft corona OVA small PS | 18.5 | 30.4 | 21.9 | 29.2 |

### 3.6. Fibril formation propensity of OVA exposed to MP

ThT fluorescence intensity upon fibril binding makes it an unusually sensitive and efficient reporter of amyloid formation. Dye binding is linked to the presence of the cross-β structure of fibrils. Ovalbumin is known to form amyloid fibrils at higher temperatures [35]. Presence of ovalbumin induced fluorescence emission of ThT, Fig. 4C suggesting presence of cross-β structure of fibrils. There were no statistically significant differences in ThT emission for all OVA samples analyzed at 25 °C, which is in agreement with stabilization of tertiary structure of bulk OVA in the presence of both PET and PS microplastics (Section 3.2). Thermally treated OVA samples, on the other hand, induced significantly higher emission of ThT, compared to non-treated samples in agreement with known propensity of OVA to form fibrils upon heating. Interestingly, thermal treatment had a similar effect on ThT emission in control OVA and bulk fraction of OVA incubated with both MPs, while heated OVA from soft corona induced significantly lower emission of ThT than heated control and bulk samples ($p < 0.05$). The result suggests that fibril formation induced by heat in soft corona OVA is affected.

### 3.7. Digestion stability of soft corona ovalbumin to pepsin and trypsin digestion

OVA is a protein known to be very resistant to trypsin and pepsin digestion. Changes in protein conformation may affect protein digestibility. Therefore, we tested OVA, as well as bulk and soft corona OVA to pepsin and trypsin digestion. Digestibility of OVA, incubated with small PS and small PET, in bulk solution and soft corona, by trypsin (after 2 min and 2 h) and pepsin (after 30 min) was not different in

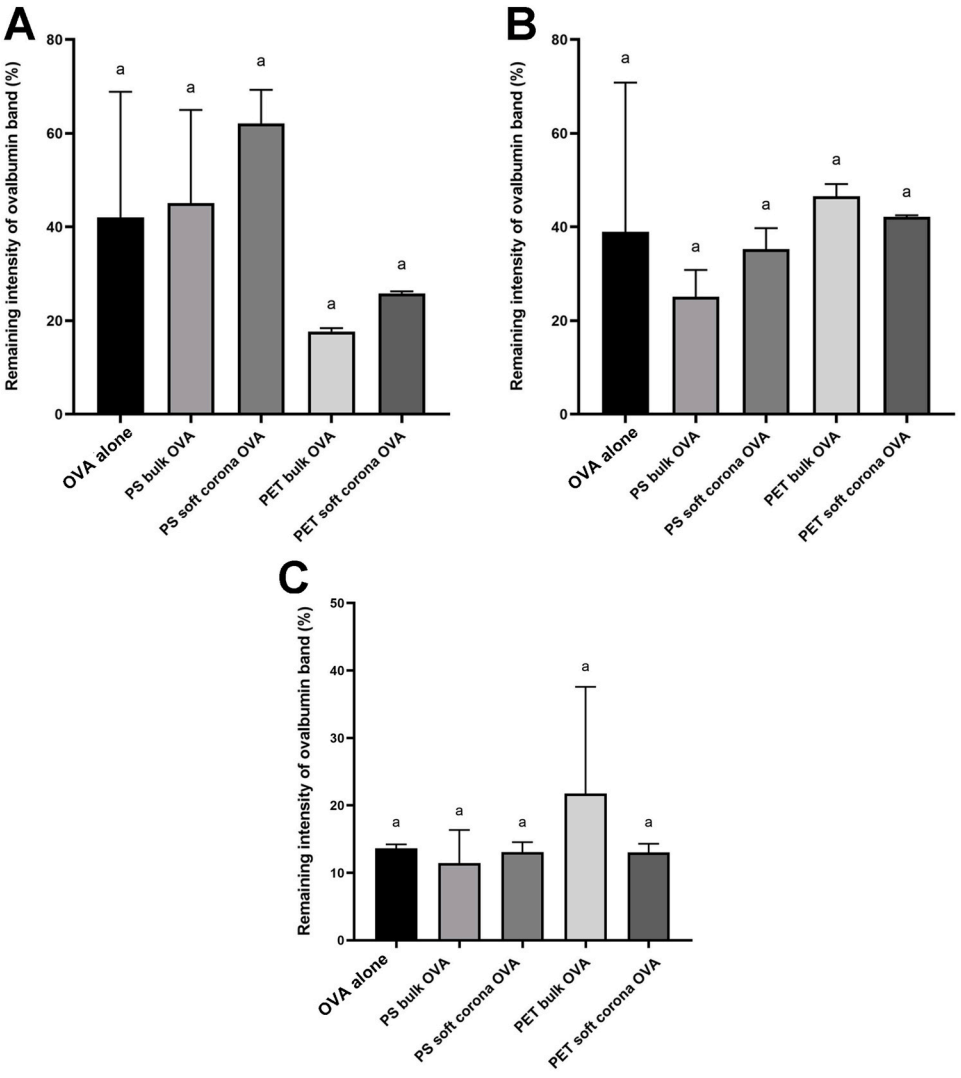


**Fig. 5.** Remaining intensity of ovalbumin (OVA) band (%) obtained by densitometry of reducing SDS-PAGE analysis of ovalbumin digestion by trypsin during 2 min (A) and 2 h (B). Remaining intensity of OVA band (%) obtained by densitometry of reducing SDS-PAGE analysis of ovalbumin digestion by pepsin (C).

comparison to native OVA (Fig. 5, **Section S5, Fig. S8**).

### 3.8. Analysis of soft and hard corona formation by egg white protein extract on the surface of MPs

The observed structural and conformational alterations in ovalbumin (OVA) following its interaction with MPs were examined using isolated proteins of high purity. To evaluate whether ovalbumin (OVA) interacts with microplastics (MPs) as effectively in the presence of other egg white proteins, we prepared an extract of egg white proteins and examined corona formation using SDS-PAGE, specifically focusing on the 40 kDa region of the gel to detect the presence of OVA. Results show that OVA in the presence of egg white protein extract forms both soft and hard corona on the surface of tested MPs under both acidic and neutral conditions, Fig. 6A and B. All three tested parameters have similar influence on OVA binding to MPs in the presence of egg white proteins, as already demonstrated with a purified OVA: MPs type, MPs size and pH. MPs with lower size adsorb higher mass of protein in both soft and hard corona, particularly at pH 3, and PS adsorbs higher mass of protein in both soft and hard corona than PET of the same size. This is in accordance with results obtained for adsorption affinity and capacity of OVA alone, e.g. small PS > small PET > large PS. However, it seems that at pH 7, higher amounts of proteins are absorbed on all tested MPs, especially considering hard corona. Particularly, lysozyme (14 kDa protein), is present only in hard corona at pH 7. Main proteins in soft corona on both pH values and in hard corona at pH 3 are ovalbumin and ovotransferrin, which is in accordance with their representation in egg white. Actually, the most dominant egg white proteins are ovalbumin (54 %), ovotransferrin (12 %), and ovomucoid (11 %), (Stevens, 1991). As ovomucoid was mostly removed during preparation of egg white protein extract, its binding could not be detected. Hard corona on pH 7 besides these two proteins contains also lysozyme and ovomucin, the next dominant egg white proteins, represented in egg white with 3.5 % and 1.5 %, respectively. Moreover, these proteins are more abundant in hard corona than in control samples, suggesting that lysozyme and ovomucin have higher affinity toward MPs than OVA and ovotransferrin. Compared to the results obtained with purified OVA (Fig. 3), OVA in the presence of egg white extract proteins seems to bind in higher amounts at pH 7 in hard corona. This suggests that the presence of other egg white proteins may influence binding of OVA to MPs at pH 7.

## 4. Discussion

Research studies on interactions between proteins and MPs, with a focus on structural and functional consequences of the interactions, is scarce. Our work provides insight into the interactions of food allergen ovalbumin and two different types of MPs (PET and PS), as well as different sizes of PS (small and large). The effect of MPs on the OVA structure and its corona formation on MPs surface was investigated, as well as the influence of thermal treatment on MPs-treated OVA. OVA corona formation was also investigated in the presence of other egg white proteins. Conditions of binding covered acidic and neutral, mimicking different pH scenarios occurring in food and during ingestion.

The protein adsorption process is considered very complex, with several stages taking place, either one after another, or simultaneously. Proteins may bind to the adsorbent irreversibly (hard corona) or reversibly (soft corona). Binding may also affect their structure, which in turn may cause additional binding to the adsorbent or spreading on its surface [36]. In addition, structural alterations of proteins may enable and facilitate mutual interactions with one another, potentially leading to formation of several protein layers onto the adsorbents. In single-protein systems, such as one applied in our study, where there is no competing adsorption among several proteins, continuous and dynamic protein adsorption and desorption occur. However, in our study there is an additional level of complexity. MP particles we studied are of very heterogeneous shapes and surfaces corresponding well to what can be found in the environment.

Several models were applied in an attempt to describe the adsorption

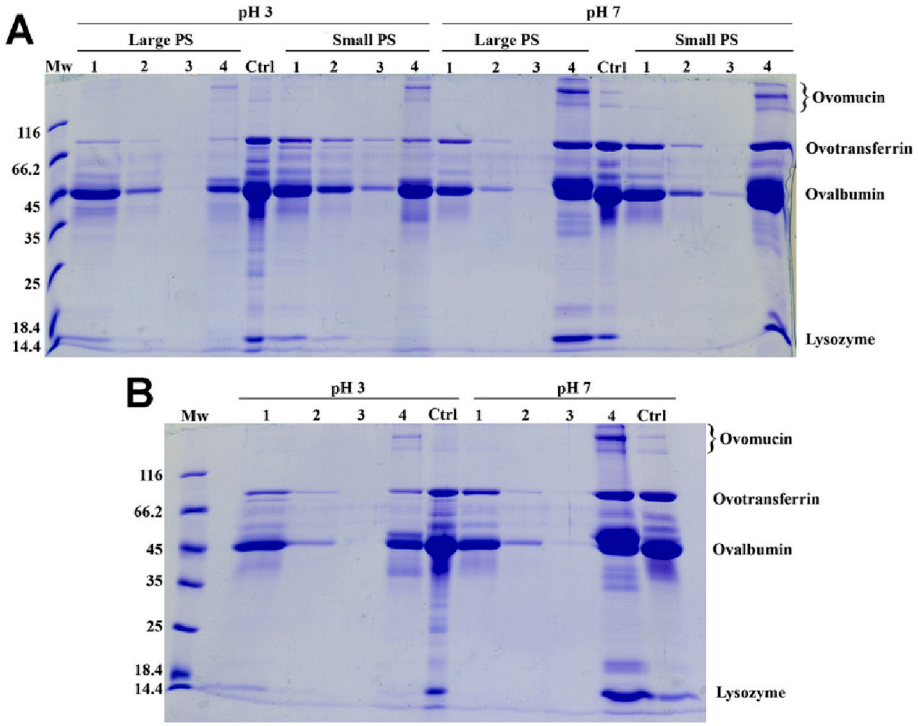


**Fig. 6.** Formation of soft and hard corona by egg white protein extract on the surface of small polystyrene and large polystyrene (A) and small polyethylene terephthalate (B), at pH 3 and 7. Lanes 1–3: egg white protein extract from soft corona, lanes 4: egg white protein extract from hard corona, Ctrl: control egg white protein extract incubated without microplastics (MPs), MW: molecular weight markers.

behavior of OVA to PET and PS as precisely as possible: Langmuir, Freundlich, RP and GAB isotherms. Langmuir model is the most, and frequently the only one used, model for analysis of adsorption equilibrium data. Although in most cases isotherm data from protein adsorption studies fit well by the Langmuir isotherm, Langmuir assumptions make this model quite inappropriate for protein adsorption [36]. There are opinions that the Langmuir model can give a valid thermodynamic description of the first interaction steps of proteins with particles [37,38]. Considering that our MPs could have a variety of OVA adsorption sites, having different adsorption energies and rates of adsorption, and that adsorbed proteins could interact between themselves, we have also used the Freundlich model [39]. Three parameter Redlich−Peterson isotherm was also used in this study as it does not assume ideal monolayer adsorption behavior, and can be used in both homogeneous and heterogeneous systems due to its versatility, combining advantages of both Freundlich and Langmuir models [40]. GAB model is a three-parameter model that can be used to describe multilayer adsorption on different areas of the surface, and assumes that the state of adsorbed molecules in the second and all higher adsorption layers is the same, but different from that in the first layer [41]. Therefore, this model is also used, as it is the most suitable for protein adsorption where protein hard and soft corona forms on the particle surface [31,32].

All four tested models provide consistent results, even though the parameter values are not exactly the same. Our experimental results fit well to Langmuir isotherm, although our experimental system does not meet any of Langmuir assumptions (monolayer adsorption, homogeneous sites, constant adsorption energy, and no lateral interaction between the adsorbed molecules). However, other three used models demonstrated that this model can provide a relatively good rough estimation of adsorption affinity and capacity. On the other hand, Langmuir isotherm cannot discriminate affinity of different sizes of PS at pH 3, in comparison to RP and GAB models, which are more appropriate for our experimental system. Similarly, Langmuir isotherm is inferior in discrimination of adsorption capacity at pH 3 and pH 7, in comparison to Freundlich model. Besides, Freundlich isotherm provides insight into system heterogeneity, while GAB isotherm is providing constant for OVA adsorption at soft corona. Using the GAB model we were not able to get reliable parameters at pH 7, most likely due to too low adsorption. It could be observed that even at pH 3 we obtained negative values of $K_{soft\ G}$ for small PET and large PS as they have lower adsorption in comparison to small PS. Therefore, for protein adsorption to MPs in general, GAB model seems to be the most relevant, providing additional $K_{soft\ G}$ constant describing adsorption and desorption between soft corona and bulk solution. However, for protein adsorption to plastic particles, the most reliable estimation of adsorption could be obtained by using several isotherm models.

In general, protein adsorption on MPs depends on type of plastics, protein sequence and conformation, particle size, particle surface, as well as conditions of adsorption determining interactions between protein and particle surface, such as pH, ionic strength and temperature. All three tested parameters determine OVA affinity and adsorption capacity: MPs size (smaller MPs > larger MPs), MPs type (for PS > PET) and pH (at pH 3 > at pH 7). Among all particles tested, the highest affinity and adsorption capacity for OVA was observed for smallest particles tested, PS, (112 μm, range 43-178 μm) at pH 3, corresponding well to the highest surface available for interaction with the protein. In the literature, only few studies have investigated binding parameters of proteins to microplastics in detail by utilizing several binding isotherms. In a study investigating interactions of pepsin with polystyrene, binding capacity of smaller particles was greater than bigger ones, and multilayered adsorption was proposed, similar to results for ovalbumin [25].

Hydrophobic interactions through the backbone and mainly π-π interactions between aromatic residues and PS phenyl rings [42] play a critical role in protein adsorption on PS particles. On the other hand, PET has a mixed alkyl and aromatic backbone to yield mildly hydrophobic properties, aromatics allowing for π-π interactions, and even carboxylate end groups adding hydrophilicity. This explains profoundly higher OVA adsorption affinity toward PS than PET. Similarly, due to higher contribution of hydrophobic surface in total MPs surface, PS MPs have also higher adsorption capacity for OVA. Small MPs have higher surface per mass unit and thus higher hydrophobic surface per mass unit, in comparison to large MPs. At pH 3, OVA is positively charged, while at pH 7 it is negatively charged (pI = 4.5). At pH 7, in absence of counter ions, carboxylate end groups dissociate and PET MPs become slightly negative. Therefore, at pH 7 slight repulsion between PET MPs and OVA could reduce the binding. For human serum albumin binding to and PVC, although binding affinity was determined by a different approach, electrostatic interactions are the main contributors to interactions [20]. PS MPs are shown to interact with lipases at pH 7 and similarly to our study, it is proposed that π–π and hydrophobic interactions are responsible for binding [43].

Several in silico binding studies have shown that PET hydrolase and manganese peroxidase are able to bind to several types of microplastics and hydrolyze them [44,45].

This is the reason why PET at pH 7 has lower adsorption affinity and capacity than at pH 3. In contrast, as PS is exclusively hydrophobic there is no repulsion between OVA and PS. That is the reason why OVA interactions with PS are stronger than with PET, particularly at pH 3. At pH 7 OVA is in its native conformation, while at pH 3 its tertiary structure is disturbed with more exposed hydrophobic regions. Therefore, for both PET and PS MPs hydrophobic interactions are more extensive at pH 3 than at pH 7. As OVA interactions with PS are hydrophobic, the difference of adsorption affinity and capacity for PS between pH 3 and pH 7 is more dramatic than the difference observed for PET. Therefore, as small PS has the highest hydrophobic surface per mass of other tested MPs, and at pH 3 OVA has higher surface hydrophobicity than at pH 7, adsorption affinity and capacity of OVA is far the highest for small PS at pH 3 in comparison to all tested MPs.

In comparison to adsorption of ions, gasses and small molecules, proteins have high molecular masses and due to conformational changes can adopt a variety of shapes, and thus a wide range of contact surface between proteins and adsorbent could be formed. Conformation of adsorbed protein molecules could enable or disable binding of another protein to neighboring sites at adsorbent surface. Besides, proteins are well known to form hard and soft layers on adsorbent. Therefore, adsorption of proteins is highly heterogeneous. Higher heterogeneity obtained for MPs with lower surface per mass is due to lower fully available surface for OVA binding per mass at higher Ce. On the other hand, at pH 3, more disturbed OVA conformation than at pH 7 is more effective in disabling binding of another protein to neighboring site at MPs surface, resulting in higher heterogeneity.

Although MPs do not change the secondary structure of bulk OVA significantly, they induce dramatic OVA tertiary structure changes, suggesting MPs-induced conformational changes due to OVA interaction with MPs. In general, at pH 3, the presence of MPs loosens OVA tertiary structure, while at pH 7 they tighten it. However, when MPs are compared, small PS has only a slight destabilizing effect at pH 3, and the most stabilizing effect at pH 7. In our previous study we have found that pepsin tertiary structure is either rigidified or maintained at pH 3 upon its adsorption to PS MPs, depending on the MPs size, influencing its activity [25].

Small PS also induces the most pronounced changes in ovalbumin secondary structure (β to α transition followed by α to β transition). In contrast, PET has the most destabilizing effect at pH 3, and the slightest stabilizing effect at pH 7, while for large PS effects are between small PET and small PS. The reason for these effects is the strongest binding of OVA to small PS. The surface of small PS is larger than of large PS, enabling more OVA molecules to adsorb, resulting in more pronounced effects. In PS, where due to steric hindrance by aromatic rings, interactions of protein residues with aliphatic areas are much lower than interactions with aromatic rings (mostly via π-π interactions), as

observed by Zhang et al. [42]. In PET there is no such hindrance, and thus aliphatic, aromatic and polar interactions with protein residues could have similar contributions. Moreover, residues exposed in proteins are more polar, thus polar interactions with PET could be a more important contributor. It seems that involvement of these polar interactions with PET is the reason for pronounced destabilizing effects of PET on OVA tertiary structure. It was reported that lipase adsorption to PS resulted in its reduced activity due to change in its secondary structure and disturbance of its open conformation essential for enzyme activity [43].

We have demonstrated that OVA forms both soft and hard corona on the surface of all three tested MPs, at both pH 3 and pH 7, and that traces of OVA fragments present in OVA preparation have higher affinity toward MPs than intact OVA. In comparison to native OVA, in soft corona OVA at pH 7, with or without heat treatment, rearrangement of α-helices and β-sheets occurred (α to β transition), and this effect was more drastic after heat treatment. However, the level of ordered secondary structures was the same as in native OVA, e.g. content of ordered secondary structure was preserved. This preserved level of ordered secondary structures in OVA from soft corona has as a consequence retained thermal stability, e.g. the same Tm as for native OVA. On the other hand, the similar content of all secondary structures in soft corona of both MPs at room temperature and in thermally treated OVA alone suggests that conformational changes in soft corona resemble conformational changes induced by heat treatment.

We have shown that also egg white protein extract forms both soft and hard corona on the surface of tested MPs, and that MPs type, MPs size and pH influence both corona formations. Adsorption of egg white proteins in corona is for small PS > small PET > large PS, which in accordance to other obtained results. However, in contrast to OVA alone, OVA in the presence of egg white extract seems to bind at higher amounts at pH 7 in soft, and particularly hard corona. It seems that, at pH 7, adsorption of other egg white proteins favors adsorption of more OVA in soft corona by protein-protein interactions, and during formation of stable hard corona more OVA are easily adsorbed to hard corona, in comparison to corona formation with OVA alone. The most represented proteins, OVA and ovotransferrin, are adsorbed in soft corona. In hard corona the next most represented proteins, lysozyme and ovomucin, are also found, having also higher affinity than OVA and transferrin, thus resulting in competitive protein adsorption. These results demonstrate that our results with isolated OVA are fully relevant for egg white as a whole food matrix. It was shown that lysozyme is able to form hard corona around PS nanoplastics (100–500 nm in size) and that this interaction promoted the primary nucleation step of amyloid fibril formation [46]. Aerogel made from hen egg-white proteins was shown to be very efficient in removing nano/microplastic contamination from seawater [47].

ThT is a structure specific molecular probe for proteins, primarily used for the detection of amyloid-like structures [48], as well as for DNA and various other biologically relevant structures [49]. ThT twisting, by intramolecular torsions around the C—C bond between benzothiazole and dimethylaniline parts, allows a change of vertically populated excited state from a locally excited to a charge-transfer state. In contrast a hindrance of this twisting, by embedding ThT into a confined space, leads to a significant decrease of the nonradiative channels with a simultaneous increase of the fluorescence [50]. In all thermally untreated samples, ThT becomes immobilized into nanopockets in OVA tertiary structure, and fluorescence is emitted. However, in heat-treated control OVA and bulk fraction of OVA incubated with both MPs, thermally induced loosening of tertiary structure enable embedding of more ThT molecules into nanocavities resulting in increased ThT emission, a propensity known to lead to fibril formation by heat treated OVA [35]. Tendency of lower ThT emission of bulk fraction of OVA incubated with MPs at 25 °C can be explained by more rigid conformation observed in near CD spectra, leaving fewer nanocavities in tertiary structure for embedding of ThT, and resulting in decreased fluorescence emission. Based on lower ThT fluorescence of heat-treated soft corona, in comparison to heated control OVA and corresponding bulk OVA, the observed conformational change in soft corona upon heat treatment, with the most dramatic α to β transition, may prevent thermally–induced loosening of tertiary structure, resulting in radiative relaxation and affect the process of fibril formation upon heat treatment. In contrast, nanoplastics seem to induce denaturation and fibrillation of proteins [51].

Given the public concern over the impact of MP and nanoplastics on the environment and living beings, more in depth studies are needed to clarify potential negative impacts of omnipresence of MPs [16]. Most of the published studies use commercially available PS MPs, of a perfectly spherical shape [12], with varying zeta-potential, which affects the behavior of PS and may influence obtained results [52]. MP particles, used in our study are made by milling process providing model particles with irregular shapes and sizes, which better corresponds to what is found in nature. However, we have investigated only two types of polymers, in a narrow range of sizes, while in the environment, a mixture of MP of various types, sizes and surface chemistries is present.

## 5. Conclusion

In this work, the binding of the main egg white protein, ovalbumin, to two types of MPs (PET and PS) of different sizes at two pH values was characterized. All three tested parameters influence MPs adsorption affinity and capacity for OVA: size (small > large), type (PS > PET) and pH (pH 3 > at pH 7). Adsorption of OVA to PS and PET MPs results in formation of soft and hard corona. Adsorption of egg white protein extract also results in the formation of soft and hard corona, where the most represented proteins, OVA and ovotransferrin, are present in both hard and soft corona. Interactions of OVA and MPs, particularly in corona, have as a consequence OVA conformational changes. Exchange of OVA between soft corona and solution results in presence of OVA molecules with altered conformation also in bulk solution. Binding of OVA to MPs affects protein structure, an important factor that determines its biological and techno-functional properties. OVA is a stable protein, and its non-native conformation adopted during interactions with MPs in soft corona is also thermally and proteolytically stable, but loses its functionality, such as amyloid fibril formation. Further research is needed to elucidate how the presence of MPs affects OVA techno-functional, nutritional and biological properties during food processing, or in vivo digestion. Particularly relevant will be to investigate effects of chronic exposure of food proteins to MPs.

## Funding

This project has received funding from the European Union's Horizon 2020 research and innovation programme under grant agreement No 965173, IMPTOX.

## CRediT authorship contribution statement

**Nikola Gligorijevic:** Writing – review & editing, Writing – original draft, Investigation, Formal analysis, Conceptualization. **Tamara Lujic:** Formal analysis, Investigation, Methodology, Visualisation, Writhing - original draft. **Tamara Mutic:** Formal analysis, Investigation, Methodology, Visualisation. **Tamara Vasovic:** Writing – review & editing, Visualization, Investigation, Formal analysis. **Maria Krishna de Guzman:** Writing – review & editing, Investigation. **Jelena Acimovic:** Writing – review & editing, Investigation. **Dragana Stanic-Vucinic:** Writing – review & editing, Writing – original draft, Visualization, Validation, Methodology, Formal analysis. **Tanja Cirkovic Velickovic:** Writing – review & editing, Supervision, Project administration, Methodology, Funding acquisition, Conceptualization.

## Declaration of competing interest

All authors confirm no conflict of interest for the publication.

## Data availability

Data are available from the University of Belgrade – Faculty of Chemistry repository of data at: http://cherry.chem.bg.ac.rs/handle/123456789/6469; https://hdl.handle.net/21.15107/rcub_cherry_6469 and http://cherry.chem.bg.ac.rs/handle/123456789/6465; https://hdl.handle.net/21.15107/rcub_cherry_6465.

## Appendix A. Supplementary data

Supplementary data to this article can be found online at https://doi.org/10.1016/j.ijbiomac.2024.131564.

## References


[1] K. Mann, M. Mann, In-depth analysis of the chicken egg white proteome using an LTQ Orbitrap Velos, Proteome Sci. 9 (2011) 7, https://doi.org/10.1186/1477-5956-9-7.

[2] M. Yamasaki, N. Takahashi, M. Hirose, Crystal structure of S-ovalbumin as a non-loop-inserted thermostabilized serpin form, J. Biol. Chem. 278 (2003) 35524–35530, https://doi.org/10.1074/jbc.M305926200.

[3] L.J. Deleu, E. Wilderjans, I. Van Haesendonck, C.M. Courtin, K. Brijs, J.A. Delcour, Storage induced conversion of ovalbumin into S-ovalbumin in eggs impacts the properties of pound cake and its batter, Food Hydrocoll. 49 (2015) 208–215, https://doi.org/10.1016/j.foodhyd.2015.03.014.

[4] S. Tufail, M.A. Sherwani, S. Shoaib, S. Azmi, M. Owais, N. Islam, Ovalbumin self-assembles into amyloid nanosheets that elicit immune responses and facilitate sustained drug release, J. Biol. Chem. 293 (2018) 11310–11324, https://doi.org/10.1074/jbc.RA118.002550.

[5] J. Costa, C. Villa, K. Verhoeckx, T. Cirkovic-Velickovic, D. Schrama, P. Roncada, P. M. Rodrigues, C. Piras, L. Martín-Pedraza, L. Monaci, E. Molina, G. Mazzucchelli, I. Mafra, R. Lupi, D. Lozano-Ojalvo, C. Larré, J. Klueber, E. Gelencser, C. Bueno-Diaz, A. Diaz-Perales, S. Benedé, S.L. Bavaro, A. Kuehn, K. Hoffmann-Sommergruber, T. Holzhauser, Are physicochemical properties shaping the allergenic potency of animal allergens? Clin. Rev. Allergy Immunol. 62 (2022) 1–36, https://doi.org/10.1007/s12016-020-08826-1.

[6] G. Martos, I. Lopez-Exposito, R. Bencharitiwong, M.C. Berin, A. Nowak-Węgrzyn, Mechanisms underlying differential food allergy response to heated egg, J. Allergy Clin. Immunol. 127 (2011) 990–997.e2, https://doi.org/10.1016/j.jaci.2011.01.057.

[7] J. Golias, M. Schwarzer, M. Wallner, M. Kverka, H. Kozakova, D. Srutkova, K. Klimesova, P. Sotkovsky, L. Palova-Jelinkova, F. Ferreira, L. Tuckova, Heat-induced structural changes affect OVA-antigen processing and reduce allergic response in mouse model of food allergy, PLoS One 7 (2012) e37156, https://doi.org/10.1371/journal.pone.0037156.

[8] Y. Li, S. Zhang, J. Ding, L. Zhong, N. Sun, S. Lin, Evaluation of the structure-activity relationship between allergenicity and spatial conformation of ovalbumin treated by pulsed electric field, Food Chem. 388 (2022) 133018, https://doi.org/10.1016/j.foodchem.2022.133018.

[9] I. Van der Plancken, A. Van Loey, M.E. Hendrickx, Foaming properties of egg white proteins affected by heat or high pressure treatment, J. Food Eng. 78 (2007) 1410–1426, https://doi.org/10.1016/j.jfoodeng.2006.01.013.

[10] H. Rostamabadi, V. Chaudhary, N. Chhikara, N. Sharma, M. Nowacka, I. Demirkesen, K. Rathnakumar, S.R. Falsafi, Ovalbumin, an outstanding food hydrocolloid: applications, technofunctional attributes, and nutritional facts, a systematic review, Food Hydrocoll. 139 (2023) 108514, https://doi.org/10.1016/j.foodhyd.2023.108514.

[11] O. Hollóczki, Evidence for protein misfolding in the presence of nanoplastics, Int. J. Quantum Chem. 121 (2021), https://doi.org/10.1002/qua.26372.

[12] K.L. Law, R.C. Thompson, Microplastics in the seas, Science (80-.). 345 (2014) 144–145, https://doi.org/10.1126/science.1254065.

[13] M. Sewwandi, H. Wijesekara, A.U. Rajapaksha, S. Soysa, M. Vithanage, Microplastics and plastics-associated contaminants in food and beverages; global trends, concentrations, and human exposure, Environ. Pollut. 317 (2023) 120747, https://doi.org/10.1016/j.envpol.2022.120747.

[14] Q. Liu, Z. Chen, Y. Chen, F. Yang, W. Yao, Y. Xie, Microplastics contamination in eggs: detection, occurrence and status, Food Chem. 397 (2022) 133771, https://doi.org/10.1016/j.foodchem.2022.133771.

[15] W.L. Shelver, A.M. McGarvey, L.O. Billey, A. Banerjee, Fate and disposition of [14C]-polystyrene microplastic after oral administration to laying hens, Sci. Total Environ. 909 (2024) 168512, https://doi.org/10.1016/j.scitotenv.2023.168512.

[16] B. Udovicki, M. Andjelkovic, T. Cirkovic-Velickovic, A. Rajkovic, Microplastics in food: scoping review on health effects, occurrence, and human exposure, Int. J. Food Contam. 9 (2022) 7, https://doi.org/10.1186/s40550-022-00093-6.

[17] M.P. Monopoli, C. Åberg, A. Salvati, K.A. Dawson, Biomolecular coronas provide the biological identity of nanosized materials, Nat. Nanotechnol. 7 (2012) 779–786, https://doi.org/10.1038/nnano.2012.207.

[18] J. Jasinski, M.V. Wilde, M. Voelkl, V. Jérôme, T. Fröhlich, R. Freitag, T. Scheibel, Tailor-made protein Corona formation on polystyrene microparticles and its effect on epithelial cell uptake, ACS Appl. Mater. Interfaces 14 (2022) 47277–47287, https://doi.org/10.1021/acsami.2c13987.

[19] A.F.R.M. Ramsperger, V.K.B. Narayana, W. Gross, J. Mohanraj, M. Thelakkat, A. Greiner, H. Schmalz, H. Kress, C. Laforsch, Environmental exposure enhances the internalization of microplastic particles into cells, Sci. Adv. 6 (2020), https://doi.org/10.1126/sciadv.abd1211.

[20] P. Ju, Y. Zhang, Y. Zheng, F. Gao, F. Jiang, J. Li, C. Sun, Probing the toxic interactions between polyvinyl chloride microplastics and Human Serum Albumin by multispectroscopic techniques, Sci. Total Environ. 734 (2020) 139219, https://doi.org/10.1016/j.scitotenv.2020.139219.

[21] P.M. Gopinath, V. Saranya, S. Vijayakumar, M. Mythili Meera, S. Ruprekha, R. Kunal, A. Pranay, J. Thomas, A. Mukherjee, N. Chandrasekaran, Assessment on interactive prospectives of nanoplastics with plasma proteins and the toxicological impacts of virgin, coronated and environmentally released-nanoplastics, Sci. Rep. 9 (2019) 8860, https://doi.org/10.1038/s41598-019-45139-6.

[22] A.P. Abad López, J. Trilleras, V.A. Arana, L.S. Garcia-Alzate, C.D. Grande-Tovar, Atmospheric microplastics: exposure, toxicity, and detrimental health effects, RSC Adv. 13 (2023) 7468–7489, https://doi.org/10.1039/D2RA07098G.

[23] H. Luo, C. Liu, D. He, J. Xu, J. Sun, J. Li, X. Pan, Environmental behaviors of microplastics in aquatic systems: a systematic review on degradation, adsorption, toxicity and biofilm under aging conditions, J. Hazard. Mater. 423 (2022) 126915, https://doi.org/10.1016/j.jhazmat.2021.126915.

[24] Z. Lett, A. Hall, S. Skidmore, N.J. Alves, Environmental microplastic and nanoplastic: exposure routes and effects on coagulation and the cardiovascular system, Environ. Pollut. 291 (2021) 118190, https://doi.org/10.1016/j.envpol.2021.118190.

[25] M.K. de Guzman, D. Stanic-Vucinic, N. Gligorijevic, L. Wimmer, M. Gasparyan, T. Lujic, T. Vasovic, L.A. Dailey, S. Van Haute, T. Cirkovic Velickovic, Small polystyrene microplastics interfere with the breakdown of milk proteins during static in vitro simulated human gastric digestion, Environ. Pollut. 335 (2023) 122282, https://doi.org/10.1016/j.envpol.2023.122282.

[26] V. Stock, C. Fahrenson, A. Thuenemann, M.H. Dönmez, L. Voss, L. Böhmert, A. Braeuning, A. Lampen, H. Sieg, Impact of artificial digestion on the sizes and shapes of microplastic particles, Food Chem. Toxicol. 135 (2020) 111010, https://doi.org/10.1016/j.fct.2019.111010.

[27] G.M. DeLoid, X. Cao, R. Coreas, D. Bitounis, D. Singh, W. Zhong, P. Demokritou, Incineration-generated polyethylene micro-nanoplastics increase triglyceride lipolysis and absorption in an in vitro small intestinal epithelium model, Environ. Sci. Technol. 56 (2022) 12288–12297, https://doi.org/10.1021/acs.est.2c03195.

[28] D.A. Omana, J. Wang, J. Wu, Co-extraction of egg white proteins using ion-exchange chromatography from ovomucin-removed egg whites, J. Chromatogr. B 878 (2010) 1771–1776, https://doi.org/10.1016/j.jchromb.2010.04.037.

[29] Worthington Biochemical Corporation, Ovalbumin - Manual. https://www.worthington-biochem.com/products/ovalbumin/manual (accessed 15 March 2023).

[30] D. Magrì, P. Sánchez-Moreno, G. Caputo, F. Gatto, M. Veronesi, G. Bardi, T. Catelani, D. Guarnieri, A. Athanassiou, P.P. Pompa, D. Fragouli, Laser ablation as a versatile tool to mimic polyethylene terephthalate nanoplastic pollutants: characterization and toxicology assessment, ACS Nano 12 (2018) 7690–7700, https://doi.org/10.1021/acsnano.8b01331.

[31] J.G. Lee, K. Lannigan, W.A. Shelton, J. Meissner, B. Bharti, Adsorption of myoglobin and Corona formation on silica nanoparticles, Langmuir 36 (2020) 14157–14165, https://doi.org/10.1021/acs.langmuir.0c01613.

[32] J. Meissner, A. Prause, B. Bharti, G.H. Findenegg, Characterization of protein adsorption onto silica nanoparticles: influence of pH and ionic strength, Colloid Polym. Sci. 293 (2015) 3381–3391, https://doi.org/10.1007/s00396-015-3754-x.

[33] M. Belhachemi, F. Addoun, Comparative adsorption isotherms and modeling of methylene blue onto activated carbons, Appl Water Sci 1 (2011) 111–117, https://doi.org/10.1007/s13201-011-0014-1.

[34] J. Ognjenović, M. Stojadinović, M. Milčić, D. Apostolović, J. Vesić, I. Stambolić, M. Atanasković-Marković, M. Simonović, T.C. Velickovic, Interactions of epigallocatechin 3-gallate and ovalbumin, the major allergen of egg white, Food Chem. 164 (2014) 36–43, https://doi.org/10.1016/j.foodchem.2014.05.005.

[35] J.M.D. Kalapothakis, R.J. Morris, J. Szavits-Nossan, K. Eden, S. Covill, S. Tabor, J. Gillam, P.E. Barran, R.J. Allen, C.E. MacPhee, A kinetic study of ovalbumin fibril formation: the importance of fragmentation and end-joining, Biophys. J. 108 (2015) 2300–2311, https://doi.org/10.1016/j.bpj.2015.03.021.

[36] R.A. Latour, The langmuir isotherm: A commonly applied but misleading approach for the analysis of protein adsorption behavior, J. Biomed. Mater. Res. Part A 103 (2015) 949–958, https://doi.org/10.1002/jbm.a.35235.

[37] S. Devineau, J.-M. Zanotti, C. Loupiac, L. Zargarian, F. Neiers, S. Pin, J.P. Renault, Myoglobin on silica: a case study of the impact of adsorption on protein structure and dynamics, Langmuir 29 (2013) 13465–13472, https://doi.org/10.1021/la4035479.

[38] S. Devineau, M. Anyfantakis, L. Marichal, L. Kiger, M. Morel, S. Rudiuk, D. Baigl, Protein adsorption and reorganization on nanoparticles probed by the coffee-ring effect: application to single point mutation detection, J. Am. Chem. Soc. 138 (2016) 11623–11632, https://doi.org/10.1021/jacs.6b04833.

[39] C.D. Hatch, J.S. Wiese, C.C. Crane, K.J. Harris, H.G. Kloss, J. Baltrusaitis, Water adsorption on clay minerals as a function of relative humidity: application of BET and Freundlich adsorption models, Langmuir 28 (2012) 1790–1803, https://doi.org/10.1021/la2042873.

[40] S. Kalam, S.A. Abu-Khamsin, M.S. Kamal, S. Patil, Surfactant adsorption isotherms: A review, ACS Omega 6 (2021) 32342–32348, https://doi.org/10.1021/acsomega.1c04661.
[41] E.O. Timmermann, A B. E. T.-like three sorption stage isotherm, J. Chem. Soc. Faraday Trans. 1 Phys. Chem. Condens. Phases 85 (1989) 1631, https://doi.org/10.1039/f19898501631.
[42] Y. Zhang, L.B. Casabianca, Probing amino acid interaction with a polystyrene nanoparticle surface using Saturation-Transfer Difference (STD)-NMR, J. Phys. Chem. Lett. 9 (2018) 6921–6925, https://doi.org/10.1021/acs.jpclett.8b02785.
[43] H. Tan, T. Yue, Y. Xu, J. Zhao, B. Xing, Microplastics reduce lipid digestion in simulated human gastrointestinal system, Environ. Sci. Technol. 54 (2020) 12285–12294, https://doi.org/10.1021/acs.est.0c02608.
[44] C.E. Duru, I.A. Duru, C.E. Enyoh, In silico binding affinity analysis of microplastic compounds on PET hydrolase enzyme target of Ideonella sakaiensis, Bull. Natl. Res. Cent. 45 (2021) 104, https://doi.org/10.1186/s42269-021-00563-5.
[45] C.E. Enyoh, T.O. Maduka, C.E. Duru, S.C. Osigwe, C.B.C. Ikpa, Q. Wang, In sillico binding affinity studies of microbial enzymatic degradation of plastics, J. Hazard. Mater. Adv. 6 (2022) 100076, https://doi.org/10.1016/j.hazadv.2022.100076.
[46] Y. Chen, Q. Liu, F. Yang, H. Yu, Y. Xie, W. Yao, Submicron-size polystyrene modulates amyloid fibril formation: from the perspective of protein corona, Colloids Surf. B: Biointerfaces 218 (2022) 112736, https://doi.org/10.1016/j.colsurfb.2022.112736.
[47] S. Ozden, S. Monti, V. Tozzini, N.S. Dutta, S. Gili, N. Caggiano, A.J. Link, N. M. Pugno, J. Higgins, R.D. Priestley, C.B. Arnold, Egg protein derived ultralightweight hybrid monolithic aerogel for water purification, Mater. Today 59 (2022) 46–55, https://doi.org/10.1016/j.mattod.2022.08.001.
[48] R. Khurana, C. Coleman, C. Ionescu-Zanetti, S.A. Carter, V. Krishna, R.K. Grover, R. Roy, S. Singh, Mechanism of thioflavin T binding to amyloid fibrils, J. Struct. Biol. 151 (2005) 229–238, https://doi.org/10.1016/j.jsb.2005.06.006.
[49] P. Hanczyc, L. Sznitko, Laser-induced population inversion in rhodamine 6G for lysozyme oligomer detection, Biochemistry 56 (2017) 2762–2765, https://doi.org/10.1021/acs.biochem.7b00243.
[50] A. Biancardi, T. Biver, B. Mennucci, Fluorescent dyes in the context of DNA-binding: the case of Thioflavin T, Int. J. Quantum Chem. 117 (2017) e25349, https://doi.org/10.1002/qua.25349.
[51] J. Windheim, L. Colombo, N.C. Battajni, L. Russo, A. Cagnotto, L. Diomede, P. Bigini, E. Vismara, F. Fiumara, S. Gabbrielli, A. Gautieri, G. Mazzuoli-Weber, M. Salmona, L. Colnaghi, Micro- and nanoplastics' effects on protein folding and amyloidosis, Int. J. Mol. Sci. 23 (2022) 10329, https://doi.org/10.3390/ijms231810329.
[52] S. Wieland, A.F.R.M. Ramsperger, W. Gross, M. Lehmann, T. Witzmann, A. Caspari, M. Obst, S. Gekle, G.K. Auernhammer, A. Fery, C. Laforsch, H. Kress, Nominally identical microplastic models differ greatly in their particle-cell interactions, Nat. Commun. 15 (2024) 922, https://doi.org/10.1038/s41467-024-45281-4.